Tradeoff Analysis of Variable Density Spiral k-Space Trajectories Used in MRI

D. Mitsouras[1], O. Afacan[2,3], D. H. Brooks[2], and F. J. Rybicki[1]

[1]Radiology, Harvard Medical School & Brigham And Women's Hospital, Boston, MA, United States, [2]Electrical And Computer Engineering, Northeastern University, Boston, MA, United States, [3]Radiology, Brigham And Women's Hospital, Boston, MA, United States

Introduction: A number of recently developed MR techniques, for applications ranging from whole-heart MRA to single-breathold coronary artery imaging and 3D spatially-selective RF excitation [1-3], employ variable density (VD) k-space trajectories, such as spirals, in order to enhance acquisition speed. In such schemes k-space sampling density is reduced below the Nyquist rate, typically as a function of distance from the center of k-space. VD trajectories are designed to extend to the same maximum k-space radius as an equivalent fixed density trajectory designed for a given image matrix size and FOV, but in a shorter duration. Consequently, the data collected does not provide sufficient information to completely resolve the imaged object without aliasing. Apart from their increasing use in MRI, the diversity of VD trajectories is also rapidly increasing, ranging from linearly and quadratically decreasing densities [1] to piecewise constant, hybrids, and even randomized trajectories [4]. Further complicating assessment of the different trajectories, a number of methods are available for image reconstruction, including standard density compensation and gridding methods [5] and extending to fast linear system solvers, such as conjugate gradient approaches, with exotic regularization schemes such as total variation minimization. Resolution, artifacts, and SNR properties can thus be affected not only by the choice of trajectory and parameters controlling the undersampling of the particular scheme, but may even be dependent on the specific parameters of the particular reconstruction used. Without a systematic comparison of different trajectories using different reconstruction methods, characterization of their tradeoffs, and hence choice for a particular application, is at best dubious. This work provides such an analysis for commonly used VD trajectory schemes as well as different reconstruction methods, based on well-founded metrics such as SNR, root-mean-square error, and point-spread function (PSF) measures such as full-width half-maximum.

Methods: Simulations were performed assuming a gradient system capable of 4 G/cm maximum amplitude and 15 G/cm/ms maximum slew rate, and the modified Shepp-Logan phantom [] as the underlying spin density. VD spiral trajectories were designed for three popular choices of the sampling density function: a) linearly decreasing [1], b) quadratically decreasing [1], and c) piecewise constant. For each choice of VD function, 100 different choices of the controlling parameter were chosen so that each trajectory generated lasted 32 ms and for the first choice of the parameter the trajectory resulted in fixed density, while the final choice of the parameter resulted in a trajectory that reached a maximum k-space radius capable of supporting the desired 22 cm FOV at a 1.87 mm spatial resolution (i.e., matrix size of 118). The parameter was smoothly varied for each scheme between the two extremes. For the piecewise constant VD scheme, two separate sets of trajectories were generated; in the first set the controlling parameter changed the k-space radius at which the trajectory switched from full density (for full 22 cm FOV) to half density (11 cm FOV), while in the second set the first quarter of the trajectory was always traversed at a full density and the parameter controlled the density of the undersampled portion. Note that a fixed density trajectory of the same duration as the trajectories generated was capable of supporting a 2.57 mm resolution (85 matrix size). That is, the most undersampled trajectory for each scheme was approximately 50% undersampled. The Shepp-Logan phantom was simulated with each trajectory 10 times, each time with a different set of noise samples added to the analytically known k-space. The noise samples were drawn from a normal distribution with std. deviation such that a fixed density trajectory would achieve an SNR of 30. For each simulation, reconstruction error was computed using the normalized root-mean-square error (NRMSE). SNR was measured using a) mean values within signal and noise ROIs and b) using the standard deviation of individual pixels over the 10 repetitions of the simulations with the different noise samples. The PSF for each trajectory was generated at a resolution of 0.02 mm. Image reconstruction was performed using a) Pipe & Menon density compensation function (DCF) [6] followed by non-uniform FFT [7], b) L_1-norm regularized linear system solution, c) Total Variation (TV) regularized linear system solution, and d) standard linear system solution (L_2-norm). For the TV-regularized case, the regularization term is the 1-norm of the 1st spatial derivative of the image. For the linear system solvers, the desired functionals were minimized using a non-linear conjugate gradient approach using the Fletcher-Reeves criteria. Since both the 1-norm and TV-norm are non-differentiable at zero, a small positive constant was used to regularize the solution.

Results: The mean NRMSE and SNR over 10 simulations, as well as the standard deviation of pixels over the 10 noisy simulations for each trajectory are shown in Fig 1 for the TV-regularized method and the Pipe & Menon DCF in Fig. 2. For each choice of the VD scheme, the line connecting the plotted points indicates the variation of the parameter controlling the undersampling. Note that each image quality metric is plotted against the full-width at half-maximum (FWHM) achieved by the respective trajectory for the respective reconstruction method. There is a somewhat non-linear relationship between the maximum k-space radius achieved by each trajectory and FWHM, particularly for quadratically decreasing VD. Accordingly, the choice of FWHM for the x-axis allows us to compare quality metrics based on the true resolution achieved by a given trajectory. It also noted that SNR measured using signal and noise ROIs is very sensitive to aliasing within the particular noise ROI and hence its location, since as a VD scheme becomes more highly undersampled (via the controlling parameter), the bulk of aliasing moves from the edge of the FOV closer to the center of the image (assuming e.g., a spin density centered in the image and fairly homogeneous). This explains the dips in SNR observed at certain FWHMs (undersampling factors). Note the small NRMSE and std. dev. difference between widely varying undersampled VD schemes for TV reconstruction.

Discussion: While the TV-regularized approach produced the best results at higher undersampling factors, it is also the most computationally expensive approach; the Pipe & Menon DCF required 4 sec to compute, and is applicable to all images for a given trajectory, while TV-regularized reconstruction required over a minute for each image. This is an issue for all linear system based reconstruction methods. For comparison, the L_2-regularized solution required about 1 sec per image, and the L_1-regularized solution required about 55 sec per image. The results strongly indicate that the choice of VD spiral trajectory undersampling scheme is not of the utmost importance when involved reconstruction methods are used. They also indicate that typical SNR measures not useful when used with VD trajectories.

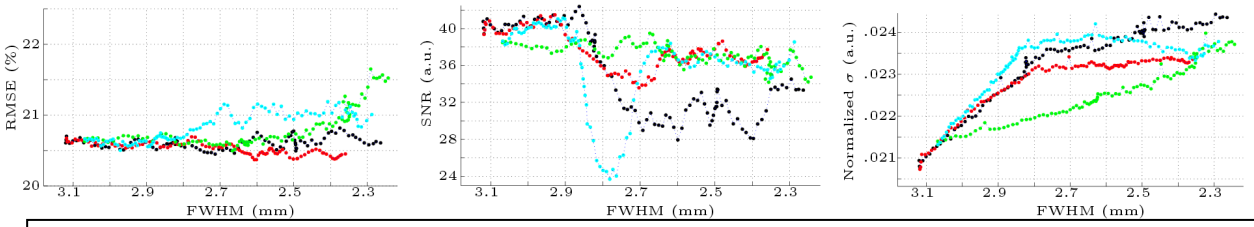

Figure 1. Top: NRMSE, SNR, and individual pixel standard deviation (over identical simulations with differing normally-distributed noise) for the 4 VD schemes considered: linearly decreasing density (black), quadratically decreasing density (red), piecewise constant with full & half density (green), and piecewise constant with full density for 1st quarter of trajectory and different fixed undersampling thereafter (cyan). **Bottom**: Same for Pipe & Menon DCF.

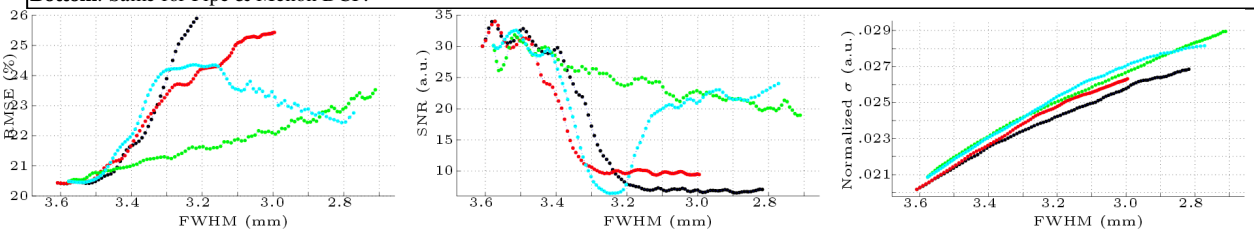

Acknowledgements: Whitaker Foundation, NIH K23-EB00882. **References:** [1] Lee at al, MRM 2003;50:1276-85. [2] Stenger et al, MRM 2003;50:1100-6. [3] Santos et al, 2006;55:371-9. [4] Lustig et al, ISMRM 2005;p.685. [5] Shepp et al, IEEE Trans Nuc Sci 1974;21:21-43. [6] Pipe et al, MRM 1999;41:179-86. [7] Fessler at al, IEEE Trans Signal Processing 2003;51:560-74